Tabu-DART: a dynamic update strategy for the Discrete Algebraic Reconstruction Technique based on tabu-search

Daniel Frenkel, Jan De Beenhouwer, and Jan Sijbers

imec-Vision Lab, Universiteit Antwerpen, Antwerp, Belgium

Abstract In X-ray Computed Tomography (XCT), the Discrete Algebraic Reconstruction Technique (DART) has been proposed as a practical method for reconstructing images measured of an object that is composed of only a small number of different materials. For such objects, DART has shown the potential to reconstruct high quality images even in the case of a low number of radiographs or a limited angular range. To this end, DART follows a set of rules to enforce the material discreteness prior knowledge. However, these rules are static in that they remain unchanged throughout the entire reconstruction process, which limits the full potential of the DART concept. To increase flexibility during the reconstruction process, we introduce an update framework that dynamically adjusts update rules throughout the iterations. Our experiments show that such dynamic update strategy leads to increased reconstruction quality and lower computational burden.

1 Introduction

In X-ray Computed Tomography (XCT), prior knowledge about the object to be reconstructed is often exploited to improve the quality of images reconstructed from limited data. A specific class of prior knowledge is the assumption that the object consists of only a small number of different materials. The domain of Discrete Tomography (DT) studies algorithms that reconstruct objects adhering to this assumption. In 2011, the Discrete Algebraic Reconstruction Technique (DART) was proposed as a practical algorithm that provides high reconstruction quality in tomographic reconstruction problems with limited X-ray projection data [1]. Since then, many variations of the DART algorithm have been reported [2–7].

The DART algorithm iteratively interchanges a reconstruction step, where the image is updated by minimizing the projection distance, and a segmentation step, where the image pixels are classified into the few different material classes. However, the rules used by DART to attribute labels to the pixels to be updated, are rigid in the sense that they do not exploit knowledge gained about the intermediate reconstructed images throughout the iterations. This slows down the algorithm or causes it to converge to a local minimum [8].

To improve upon the rigid DART update rules, we propose a generalization of the DART update strategy by introducing a dynamic update probability map of the image throughout the reconstruction. We express update strategies as changes to the update probability map and we exploit the probability map sequence by using a tabu-search framework. We show that this approach improves both convergence speed and reconstruction quality.

2 Materials and Methods

2.1 The DART algorithm

DART assumes that the object to be scanned consists of a small number (typically $k < 5$) of different materials. Let $\{\rho_1 < ... < \rho_k\}$ be the gray values representing the different materials present in the object and $\mathbf{x} \in \mathbb{R}^n$ the representation of the pixel grid of attenuation values of the object. Given the measured projection data $\mathbf{p} \in \mathbb{R}^m$ and the system matrix $\mathbf{W} \in \mathbb{R}^{m \times n}$, the reconstruction problem comes down to solving the linear system

$$\mathbf{W}\mathbf{x} = \mathbf{p}, \quad \text{such that } \mathbf{x} \in \{\rho_1, .., \rho_k\}^n. \tag{1}$$

To this end, the following steps are performed in the DART algorithm: First, an initial reconstruction is calculated with the use of an Algebraic Reconstruction Method (ARM), such as ART, SART or SIRT [9]. Without loss of generality, we will use the SIRT algorithm as the ARM. The output vector is denoted as $\mathbf{x}^{(0)}$. Since the output of an ARM has continuous gray values, which violates the discreteness assumption, a segmentation step is performed to enforce discreteness. Similar to [1], we use a global thresholding step with the following mapping function:

$$S(\mathbf{x}, \rho) : \mathbb{R}^n \longrightarrow \{\rho_1, \rho_2, ..., \rho_k\}^n \ \mathbf{x} \rightarrow \mathbf{s},$$

$$s_i = \begin{cases} \rho_1, & x_i < \tau_1 \\ \rho_2, & \tau_1 \leq x_i < \tau_2 \\ \vdots & \\ \rho_k, & \tau_{k-1} \leq x_i, \end{cases} \qquad i = 1, ..., n,$$

where the thresholds τ_j are calculated as

$$\tau_j = \frac{\rho_j + \rho_{j+1}}{2}, \ j = 1, ..., k-1. \tag{2}$$

The resulting discrete image is denoted as $\mathbf{s}^{(0)} = S(\mathbf{x}^{(0)})$. Let $\mathbf{s}^{(\ell)}$ be the segmentation from the ℓ-th iteration of DART. First, all pixels in $\mathbf{s}^{(\ell)}$ classified either as boundary or interior pixels. A pixel is considered interior when it belongs to the same material class as its neighbours. All other pixels are considered boundary pixels. Only the boundary pixels are updated in the next ARM iteration while interior regions are kept fixed. Let $(\mathbf{w_1}, ..., \mathbf{w_n})$ be the columns of the system matrix $\mathbf{W}$. The boundary pixels are reconstructed on the

residual data:

$$\mathbf{W}_{(\ell)}\mathbf{x}^{(\ell)} = \mathbf{p} - \mathbf{w_i} s_i^{(\ell)}, \tag{3}$$

$$\mathbf{W}_{(\ell)} = (\mathbf{w_1}, \ldots, \mathbf{w_{i-1}}, \mathbf{w_{i+1}}, \ldots, \mathbf{w_n}), \tag{4}$$

$$\mathbf{x}^{(\ell)} = (x_1, ..x_{i-1}, x_{i+1}, .., x_n)^T \tag{5}$$

To minimize the risk of local minima, each interior pixel also has a probability p of being included in the next reconstruction step. Solving the reduced system (3) yields a new vector containing updated values for the boundary pixels and the fixed pixels that were randomly selected. Along with the fixed pixels, a new image $\mathbf{x}^{(\ell+1)}$ is computed. Finally, a smoothing operation is performed by convolving the image with a 3×3 mean kernel.

The above process is repeated until a convergence criterion is met or a predetermined maximum number of DART iterations is reached.

2.2 The Tabu-search concept

Tabu-search is a mathematical optimization method that employs a memory structure to improve local search methods. By manipulating adaptive memory structures, Tabu-search methods can reach parts of the solution space that would otherwise have been left unexplored by more traditional methods. There exist many variations that characterize the memory structure in Tabu-search [10]. However, one of specific interest for the DART update rules is frequency based memory. This variant contains and uses information on the amount of times a certain attribute has appeared in recent solutions. If the presence of a property is correlated to good solutions, then remembering search directions where many solutions with this property exist increases the probability of finding an optimal solution. There are various metrics that we can track about a reconstruction that change once the DART algorithm nears convergence. An example of that would be how many pixels still change their material class. By measuring the class change for each pixel individually, we essentially create a frequency based memory structure related to the material labeling of the image. We can exploit changes in this structure to adapt the DART algorithm update step. In this way, the solution guiding process becomes more refined over time.

In the next section, we will generalize the DART update step as a framework which uses a probability map to function as a frequency based memory structure for the update step inside the algorithm as shown in Figure 1. We will also describe an algorithm called Tabu-DART, which uses a dynamic set of rules to update the probability map. By changing the values of the probability map, we directly influence the frequency with which individual pixels are updated in the following iterations.

2.3 Tabu-DART: using a probability map to function as memory for DART

Tabu-search is a heuristic technique which uses the concept of memory to increase control of the solution space. We implemented this concept in the DART update step because it directly relates to both convergence speed and reconstruction quality of the DART algorithm. In [1], this step is based on a boundary criterion and a probability parameter p for each pixel. Instead of one parameter p describing the probability that an interior pixel is updated in the next iteration, Tabu-DART uses a map:

$$P : \mathbb{R}^n \longrightarrow [0,1]^n, \mathbf{x} \longrightarrow \mathbf{p_x} \tag{6}$$

As such, each pixel in the image has its own unique probability and for each pixel it is individually decided whether or not it is updated in the next iteration. The Tabu-DART can be summarized as follows:

1. After an initial segmentation, the probability map $\mathbf{p}_\mathbf{x}^{(\ell)}$ is initialized.
2. During the partitioning step, a random value $r_i^{(\ell)}$ between 0 and 1 is generated for each pixel $x_i^{(\ell)}$. If $r_i^{(\ell)} \leq p_{x_i}^{(\ell)}$, then the pixel is selected for update.
3. At the end of every DART iteration, a feedback step is added that updates the probability map based on changes between the new segmented image and the one found in the previous DART iteration. In this way, the probability map adapts quickly to changes in the reconstructed image.

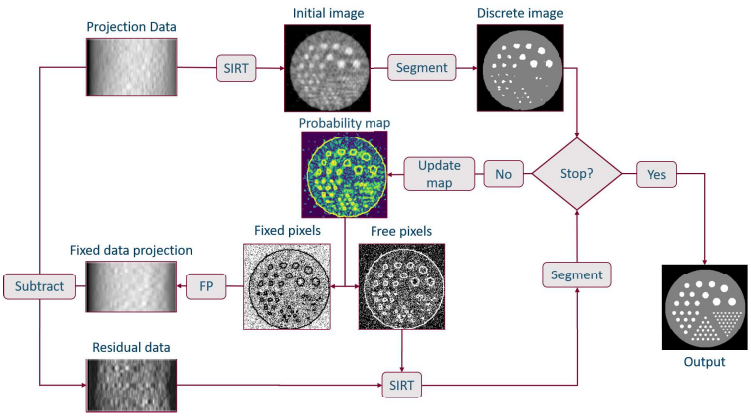

Figure 1: A flowchart of the Tabu-DART algorithm.

Note that this framework encloses the original DART algorithm [1] with random parameter p and segmentation $s^{(\ell)}$ as follows:

$$p_{x_i}^{(\ell)} = \begin{cases} 1, & \text{if } s_i^{(\ell)} \text{ is boundary} \\ p, & \text{if } s_i^{(\ell)} \text{ otherwise} \end{cases} \qquad i = 1, \ldots, n. \tag{7}$$

We decided on a different approach in Tabu-DART. Each pixel x_j is linked to a probability vector of length k representing the probabilities that x_i belongs to each material class.

We denote this vector by $\mathbf{v}_{x_j}$. By using the entropy

$$\mathscr{H}(x_j) = -\mathbf{v}_{x_j}^T \log_2(\mathbf{v}_{x_j}), \tag{8}$$

a single value representing uncertainty of the pixel x_i can be calculated. Varga et al. [11] described a method to calculate the entropy for binary images. Let y_j be the value of pixel x_j as a result of the initial ARM iterations. Then, the probability vector $\mathbf{v}_{x_j}$ for a pixel x_j is defined

$$\mathbf{v}_{x_j} = [y_j, 1-y_j],$$

and this becomes the input into (8). However, this approach is applicable only to binary images. As to generalize it to more than two classes, we suggest the following for the output $\mathbf{y}$ from the ARM. Let

$$\mathbf{d}_{x_i} = \left[\frac{1}{|y_i-\rho_0|}, \ldots, \frac{1}{|y_i-\rho_k|}\right]$$
$$\mathbf{v}_{x_i} = \frac{\mathbf{d}_{x_i}}{\|\mathbf{d}_{x_i}\|_1}$$

The resulting vector $\mathbf{v}_{x_i}$ is input into (8) to yield a single value $\mathscr{H}(x_i)$ measuring uncertainty for the pixel x_i. These uncertainty values are used to initialize the probability map. The probability map update step is also different and based on three rules:

1. A pixel changing class during the last DART iteration, indicates that the uncertainty of which class it belongs to is still high. To ensure that the pixel will be updated again in the next iteration, its update probability is set to 1.

2. When a pixel did not change material classes compared to the last DART iteration, its corresponding update probability is halved instead. In this way, stable regions are iteratively removed from the reconstruction problem.

3. As was pointed out in [1], the boundary plays a key role as it holds the most uncertainty in the image. the update probability of each boundary pixel is set to 1 as in [1].

3 Experiments and Results

3.1 Simulation experiments

To evaluate the effect of the proposed dynamic update strategy on the reconstruction quality, we simulated projection datasets of a laminate profile phantom (Figure 2) with decreasing angular range with a geometry that represents the one used when scanning objects in the UAntwerp FlexCT scanner [12]. We assumed a monochromatic beam with fan-beam geometry with a phantom size of 200×400, a Source-Object-Distance (SOD) of 360 mm and a Source-Detector-Distance (SDD) of 90 mm. The voxel size was set to 0.120 mm. We varied the angular range from 40 to 140 degrees, with the number of projections taken varying from 20 up to 70. The simulation was performed with the ASTRA toolbox [13]. Simulated Poisson noise with an average photon count of 25000 was added to the projection data. The reconstruction was performed using both the DART and Tabu-DART algorithms described in Section 2. In addition, we implemented the ADART algorithm [2] and a variant of it employing the Tabu-DART based map update. The update step for ADART is given by:

$$P^k(x_i, s) = \begin{cases} 1 & \text{if } i \in B_s^k \\ p & \text{if } i \notin B_s^k, \end{cases}$$

where the boundary set $B_s^{(k)}$ changes over time. A total of 50 initial SIRT iterations were run, followed by 95 DART iterations. Following the original paper [1], each DART iteration contained a subroutine of 10 masked SIRT iterations, the value for p for DART and ADART was set to 0.15, and the smoothing factor was set to 0.1. This amounts to 1000 SIRT iterations for each method. To counteract the effects of noisy data, a relaxation factor λ was introduced to the SIRT algorithm in the following way:

$$\mathbf{x}^{(k+1)} = \mathbf{x}^{(k)} + \lambda \mathbf{C}\mathbf{W}^\top \mathbf{R}(\mathbf{p} - \mathbf{W}\mathbf{x}^{(k)}), \tag{9}$$

where each DART iteration λ was set to the number of free pixels divided by the total number of pixels. To measure the performance of the methods, we calculate the number of misclassified pixels, denoted as the *pixel error*.

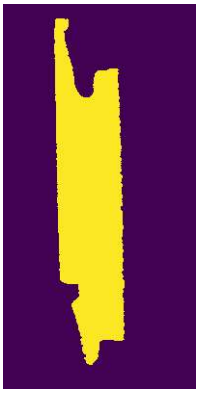

Figure 2: The Laminate phantom used in the experiment

3.2 Simulation results

Figure 3 shows the pixel error as a function of the angular range for the four DART methods described in the previous section and the average relaxation factor λ. These errors have been averaged over 50 repetitions with different seeds for the generation of the Poisson noise. We observe a lower pixel error for the algorithms based on Tabu-search compared to the original methods (DART and ADART) for each choice of angular range. The reconstructions are shown in Figure 4. The visual difference, however, is negligible. The relaxation factor in this experiment was set to reflect the number of freed pixels. These directly influence the computational cost

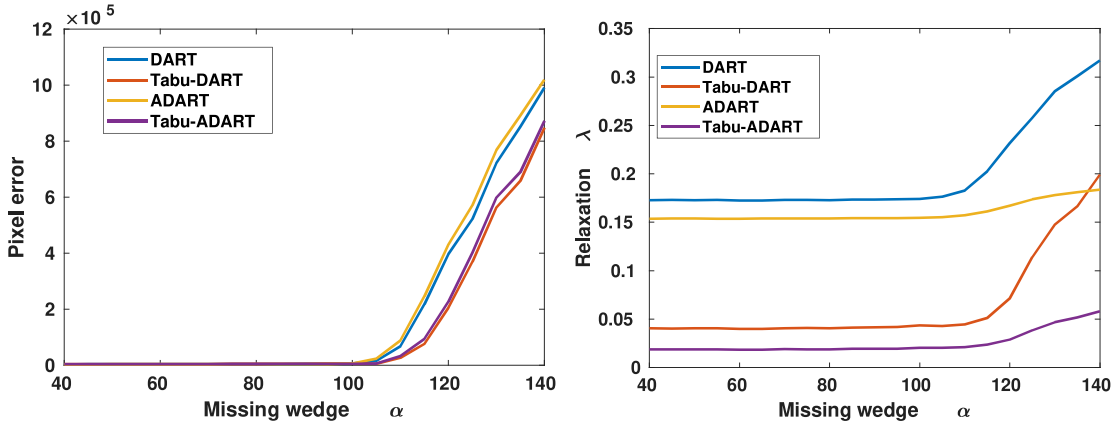

Figure 3: The pixel error as a function of the angular range for the laminate phantom (left) and the average relaxation factor (right). Tabu-DART and Tabu-DART start outperforming DART and ADART once the missing wedge becomes large. The relaxation factor represents the system size and indicates where the algorithm performance starts deteriorating.

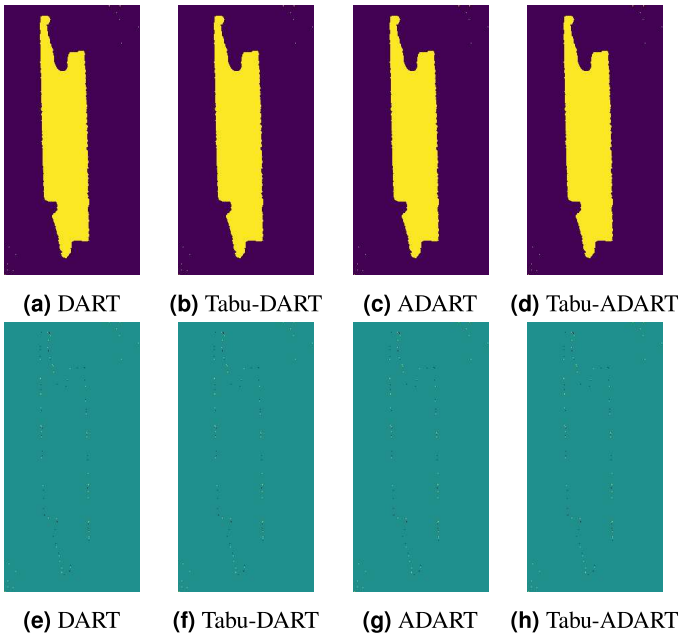

(a) DART **(b)** Tabu-DART **(c)** ADART **(d)** Tabu-ADART

(e) DART **(f)** Tabu-DART **(g)** ADART **(h)** Tabu-ADART

Figure 4: Reconstruction for a 100 ° angular range. The first row (a-d) shows the laminate image resulting from the methods. The second (e-h) row shows difference images with the phantom. While there is a difference in pixel error, the visual difference is negligible.

of performing the DART iterations, and are lowest for Tabu-DART and Tabu-ADART. Our approach allows for a lower pixel error and similar visual quality at a lower computational cost. A sudden increase of λ can be observed for all methods once the removed wedge increases past 110°. This indicates the breaking point of the DART algorithm, reconstruction becoming more and more unreliable past this point.

4 Conclusion

We have introduced a new update strategy which generalizes the rigid update rules that DART and some of its variants use in subsequent iterations. By representing the update strategy with a probability map we yield more dynamic control of the reconstruction regions and even singular pixels. The specific example of the framework that we presented is however far from optimal. Because of the flexibility of the framework it is possible to introduce complex selection methods that are based on priors already used in other methods such as Total Variation minimization (TV) algorithms, statistical reconstruction methods, or even learned priors. This is a subject of our further work.

5 Acknowledgements

This research is funded by the FWO SBO project MetroFlex (S004217N).

References

[1] K. J. Batenburg and J. Sijbers. “DART: a practical reconstruction algorithm for discrete tomography”. *IEEE Transactions on Image Processing* 20.9 (2011), pp. 2542–2553.

[2] F. J. Maestre-Deusto, G. Scavello, J. Pizarro, et al. “ADART: An adaptive algebraic reconstruction algorithm for discrete tomography”. *IEEE Transactions on image processing* 20.8 (2011), pp. 2146–2152.

[3] J. Liu, Z. Liang, Y. Guan, et al. “A modified discrete tomography for improving the reconstruction of unknown multi-gray-level material in themissing wedge’situation”. *Journal of synchrotron radiation* 25.6 (2018), pp. 1847–1859.

[4] E. Demircan-Tureyen and M. E. Kamasak. “A discretized tomographic image reconstruction based upon total variation regularization”. *Biomedical Signal Processing and Control* 38 (2017), pp. 44–54.

[5] X. Zhuge, W. J. Palenstijn, and K. J. Batenburg. “TVR-DART: a more robust algorithm for discrete tomography from limited projection data with automated gray value estimation”. *IEEE Transactions on Image Processing* 25.1 (2015), pp. 455–468.

[6] L. F. A. Pereira, E. Janssens, G. D. Cavalcanti, et al. “Inline discrete tomography system: Application to agricultural product inspection”. *Computers and electronics in agriculture* 138 (2017), pp. 117–126.

[7] A. Dabravolski, K. J. Batenburg, and J. Sijbers. "A multiresolution approach to discrete tomography using DART". *PloS one* 9.9 (2014), e106090.

[8] D. Frenkel, J. Beenhouwer, and J. Sijbers. "An adaptive probability map for the Discrete Algebraic Reconstruction Technique". *10th Conference on Industrial Computed Tomography (iCT),(iCT 2020) Wels, Austria*. 2020, pp. 4–7.

[9] A. C. Kak, M. Slaney, and G. Wang. "Principles of computerized tomographic imaging". *Medical Physics* 29.1 (2002), pp. 107–107.

[10] F. Glover and M. Laguna. "Tabu search: effective strategies for hard problems in analytics and computational science". *Handbook of Combinatorial Optimization* 21 (2013), pp. 3261–3362.

[11] L. G. Varga, L. G. Nyúl, A. Nagy, et al. "Local and global uncertainty in binary tomographic reconstruction". *Computer Vision and Image Understanding* 129 (2014), pp. 52–62.

[12] B. De Samber, J. Renders, T. Elberfeld, et al. "FleXCT: a flexible X-ray CT scanner with 10 degrees of freedom". *Opt. Express* 29.3 (2021), pp. 3438–3457. DOI: 10.1364/OE.409982.

[13] W. Van Aarle, W. J. Palenstijn, J. De Beenhouwer, et al. "The ASTRA Toolbox: A platform for advanced algorithm development in electron tomography". *Ultramicroscopy* 157 (2015), pp. 35–47.

[14] W. Van Aarle, K. J. Batenburg, and J. Sijbers. "Automatic parameter estimation for the Discrete Algebraic Reconstruction Technique (DART)". *IEEE Transactions on Image Processing* 21 (2012), pp. 4608–4621. DOI: 10.1109/TIP.2012.2206042.